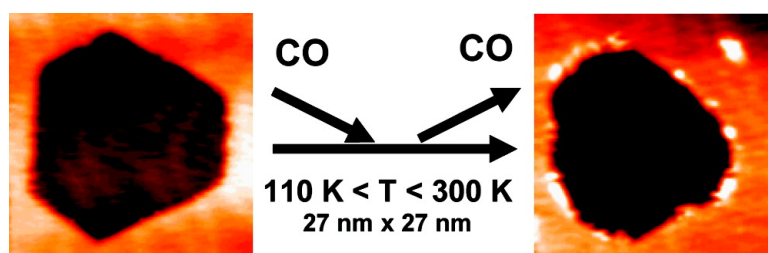


Adsorbate-Driven Morphological Changes of a Gold Surface at Low Temperatures

Jan Hrbek, Friedrich M. Hoffmann, Joon B. Park, Ping Liu, Dario Stacchiola, Yong
 Soo Hoo, Shuguo Ma, Akira Nambu, Jose A. Rodriguez, and Michael G. White

J. Am. Chem. Soc., **2008**, 130 (51), 17272-17273 • DOI: 10.1021/ja8081268 • Publication Date (Web): 02 December 2008

Downloaded from <http://pubs.acs.org> on February 8, 2009



More About This Article

Additional resources and features associated with this article are available within the HTML version:

- Supporting Information
- Access to high resolution figures
- Links to articles and content related to this article
- Copyright permission to reproduce figures and/or text from this article

[View the Full Text HTML](#)

Adsorbate-Driven Morphological Changes of a Gold Surface at Low Temperatures

Jan Hrbek,^{*} Friedrich M. Hoffmann,[†] Joon B. Park, Ping Liu, Dario Stacchiola, Yong Soo Hoo,[‡] Shuguo Ma,[§] Akira Nambu,[⊥] Jose A. Rodriguez, and Michael G. White^{||}
Chemistry Department 555, Brookhaven National Laboratory, Upton, New York 11973

Received October 15, 2008; E-mail: hrbek@bnl.gov

The notion of active site in heterogeneous catalysis as a static configuration of low-coordination surface atoms is being replaced by the concept of dynamic active site.^{1,2} This idea is directly supported by a growing number of experimental and theoretical results.^{3,4} For example, gold surfaces are undergoing significant restructuring in the presence of reactants or even weakly adsorbed molecules.^{5–7} Current interest^{8–10} in the reactivity of gold has its origin in discoveries of gold catalytic properties two decades ago.^{11,12} The unprecedented catalytic activity of supported Au nanoparticles in the low temperature CO oxidation^{9,10,12} stands in sharp contrast to the limited reactivity of the close-packed (111) surface of this noble metal. Present understanding is that CO adsorption requires the presence of low-coordination sites provided by stepped or more open surfaces of gold.^{13–16} To adsorb CO on the Au(111) surface high CO pressures (>1 torr) are needed, but adsorption drives surface restructuring and roughening.^{17–19}

In this Communication we demonstrate that CO adsorption on the Au(111) surface can be increased by controlling the length of steps,²⁰ and that the weakly adsorbed CO induces irreversible morphological changes of the surface even at temperature below 180 K and very low CO pressures (5×10^{-9} torr).

The modified Au(111) surfaces were characterized by scanning tunneling microscopy (STM) and CO adsorption was monitored by infrared reflection absorption spectroscopy (IRAS).²¹ Infrared spectroscopy has extremely high sensitivity for CO and CO itself is a very sensitive probe of adsorption sites. Density functional theory (DFT) calculations were used to rationalize the experimental results.

CO adsorption on the well-annealed Au(111) surface is largely suppressed, as shown in Figure 1, curve set A. Depending on the final annealing conditions during sample preparation, only a very weak broadband at 2115–2110 cm^{-1} is observed. On the basis of the observed absorption intensity (~ 0.0001 AU), we estimate a surface coverage of $\theta \leq 0.002$, which we attribute to adsorption on monatomic steps of the "smooth" Au(111). The observation that CO coverage on the annealed Au(111) is very limited at low pressures and temperatures is in agreement with earlier work.^{13,14}

Introducing surface defects drastically increases the amount of adsorbed CO. The gold surface patterned by one atomic layer deep vacancy islands, shown in Figure 2, reveals a significant increase in the overall number of monatomic steps. Figure 2 demonstrates that we can control the step length while preserving the structural integrity of the surface, as evidenced by the preservation of the herringbone reconstruction of Au(111) after sputtering at 400 K. Most of the hexagonal islands visible in Figure 2 are bordered by monatomic steps running along the close-packed $\langle 100 \rangle$ directions

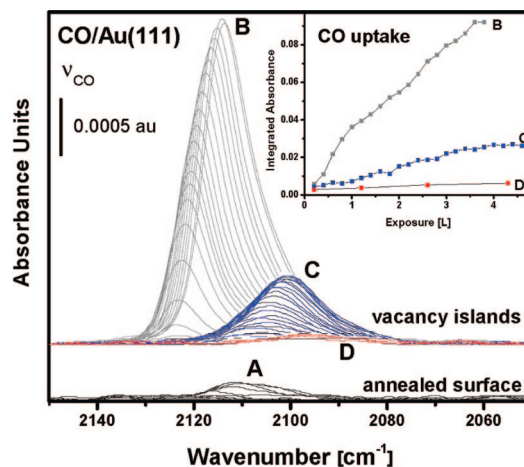


Figure 1. Comparison of CO adsorption IR spectra at ~ 110 K on smooth (A) and patterned (B, C, D) gold surfaces. Readsorption data (C, D) display significant decrease of CO uptake (inset).

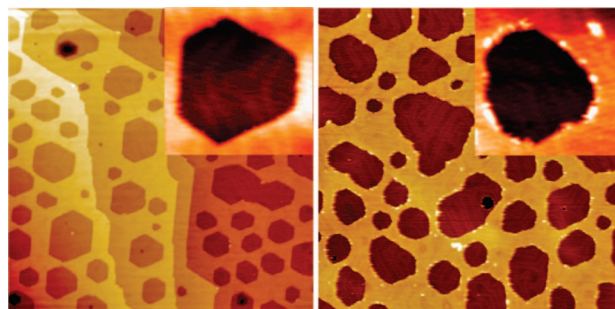


Figure 2. Room temperature STM images ($200 \text{ nm} \times 200 \text{ nm}$; $27 \text{ nm} \times 27 \text{ nm}$ inset) of the vacancy islands modified Au(111) surface before CO adsorption (left) and after CO adsorption-desorption cycle (right).

thus extending the step length of the smooth surface more than 10-fold after patterning.

IR data, acquired during CO adsorption on the patterned gold surface show a drastic increase in the amount of adsorbed CO (gray curves, set B and inset in Figure 1). The vibrational spectra are characterized by a single C–O stretch, which shifts with increasing coverage from 2124 to 2114 cm^{-1} . The peak intensity at saturation is almost 20 times higher than that of the smooth surface. This increase in CO saturation coverage is found to follow the increase in the overall step length for the patterned surface.

The C–O stretch frequency and its coverage-dependent shifts are in agreement with earlier data reported for Au(332)¹⁴ and modified Au(111).¹⁵ The continuous red shift in the IR data indicates repulsive interaction among adsorbed molecules, a behavior consistent with the absence of the CO islands formation.²¹ We argue that the CO repulsive interactions require adsorption at

[†] Department of Science, BMCC-CUNY, New York, NY 10007.

[‡] Department of Chemistry, Marquette University, Milwaukee, WI 53201.

[§] College of Engineering and Computing, USC, Columbia, SC 29208.

[⊥] Advanced Research Laboratory, Hitachi Ltd, Saitama 350-0395 Japan.

^{||} Department of Chemistry, SUNY, Stony Brook, NY 11794.

1D surface motifs such as steps. Readsorption of CO after thermal desorption revealed irreversible surface changes due to the previous adsorption–desorption cycle. After thermal desorption of CO (maxima at 135 and 185 K) the Au sample was cooled and CO adsorption repeated under the same conditions. Results are shown in Figure 1 (blue curves, set C). There is a substantial (72%) decrease in IR intensity at saturation and a downshift in the range of C–O stretch frequencies (2107–2100 cm^{-1}). The second readsorption (Figure 1, red curves, set D) has an even more drastic impact on the spectra: we see only 7% of the original intensity and the C–O stretch is found at a fixed position of 2097 cm^{-1} . The IR data indicate that repeated adsorption–desorption of CO leads to quantitative and qualitative changes of the adsorption sites: the original sites decrease in number first and then disappear. Judging from the C–O stretch frequency and a lack of any frequency shifts with exposure, CO appears to generate very few new and isolated adsorption sites. Interestingly, similar frequencies around 2100 cm^{-1} were reported for CO adsorbed on oxide supported gold nanoparticles.^{22,23}

STM images obtained before and after adsorption–desorption cycles (see Figure 2) show that the vacancy islands lost their original hexagonal shape with well-defined straight steps. Most of them acquired a round form and in addition are decorated by nanosized particles attached to the upper step edge. The herringbone reconstruction of the surface is preserved. A line profile suggests that these features are made of 0.2 nm high nanoparticles with diameters about 1 nm. Annealing the surface to 400 K removes nanoparticles and restores the original hexagonal shape of the vacancy islands. We therefore conclude that weakly adsorbed CO facilitates the mobility of Au adatoms on the close-packed surface even at temperatures below 273 K.

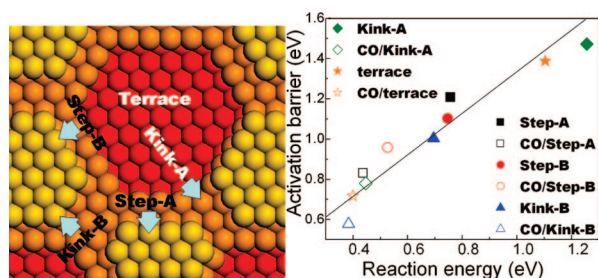


Figure 3. (left) Ball model of the modified Au(111) surface with five adsorption sites labeled; (right) plot comparing the reaction energies vs reaction barriers for a climb of an Au atom from five different sites to the upper terrace before and after CO adsorption.

DFT calculations^{24,25} were carried out to understand the effect of CO adsorption on the morphology of Au(111). To simulate the vacancy islands prepared experimentally, five different sites were considered (Figure 3): Au(111) terrace, step-A ($\{100\}$ -faceted), Step-B ($\{111\}$ -faceted), Kink-A, and Kink-B. Our results show that CO prefers the low-coordinated Au sites and the CO–Au binding becomes weaker when moving from Kink-B (−1.20 eV) to Step-A (−0.90 eV), Step-B (−0.87 eV), Kink-A (−0.35 eV), and to the terrace site (−0.31 eV), as the coordination number of the Au site increases from 6 to 9. A similar trend was also observed for the migration of an Au atom as seen in Figure 3, where we plot the reaction energy vs reaction barrier for moving an Au atom from five different sites to the upper terrace with or without adsorbed CO. One can see that the reaction energy and the barrier are well correlated: the more endothermic the reaction energy is, the higher the corresponding barrier will be. Again, the calculations show that the low-coordinated Au atoms at Kink-B, Step-A, and Step-B climb

more easily to the upper terrace than the high-coordinated atom at the terrace and Kink-A sites. However, in the absence of CO, these movements are highly activated with the barriers higher than 1 eV, and therefore very unlikely at the low temperature condition of the experiment. In contrast, when CO is adsorbed, moving an Au atom is less endothermic and the barrier is correspondingly lowered. Compared to the bare surface, CO adsorption elongates the Au–Au bond and consequently weakens the Au–Au interaction. It also stabilizes the addition of Au atoms to the upper terrace and facilitates their migration. Limited CO adsorption at the curved island boundaries can then be associated with an increase of the less favorable Kink-A sites that are replacing the straight boundaries. Overall, DFT results support experimental observations that CO enhances the mobility of Au and restructures the Au(111) surface.

In summary, we have demonstrated that low temperature adsorption of CO on a gold surface modified by hexagonal vacancy islands results in transformation of the hexagonal islands to the round ones and the formation of nanosized Au particles. This observation points to the dynamic response of surfaces to even weakly adsorbing reactants during catalytic reactions.

Acknowledgment. This research was carried out at Brookhaven National Laboratory and supported by the US DOE (Chemical Sciences Division, Grant DE-AC02-98CH10886).

References

- (1) Ertl, G. *Faraday Discuss.* **2002**, *121*, 1.
- (2) Somorjai, G. A.; Marsh, A. L. *Philos. Trans. R. Soc., A* **2005**, *363*, 879.
- (3) Nakagoe, O.; Watanabe, K.; Takagi, N.; Matsumoto, Y. *Phys. Rev. Lett.* **2003**, *90*, 226105.
- (4) Newton, M. A.; Belver-Colderira, C.; Martinez, Arias, A.; Fernandez-Garcia, M. *Nat. Mater.* **2007**, *6*, 528.
- (5) Driver, S. M.; Zhang, T.; King, D. A. *Angew. Chem., Int. Ed.* **2007**, *46*, 700.
- (6) Giorgio, S.; Cabie, M.; Henry, C. R. *Gold Bulletin* **2008**, *41*, 167.
- (7) Baber, A. E.; Jensen, S. C.; İski, Z. E. V.; Sykes, E. C. H. *J. Am. Chem. Soc.* **2006**, *128*, 15384.
- (8) Ojifinni, R. A.; Froemming, N. S.; Gong, J.; Pan, M.; Kim, T. S.; White, J. M.; Henkelman, G.; Mullins, C. B. *J. Am. Chem. Soc.* **2008**, *130*, 6801.
- (9) Turner, M.; Golovko, V. B.; Vaughan, O. P. H.; Abdulkin, P.; Berenguer-Mutcia, A.; Tikhov, M. S.; Johnson, B. F. G.; Lambert, R. M. *Nature* **2008**, *454*, 981.
- (10) Herzing, A. A.; Kiely, C. J.; Carley, A. F.; Landon, P.; Hutchings, G. J. *Science* **2008**, *321*, 1331.
- (11) Hutchings, G. J. *J. Catal.* **1985**, *96*, 292.
- (12) Haruta, M.; Kobayashi, T.; Sano, H.; Yamada, N. *Chem. Lett.* **1987**, 405.
- (13) Dumas, P.; Tobin, R. G.; Richards, P. L. *Surf. Sci.* **1986**, *171*, 579.
- (14) Ruggiero, C.; Hollins, P. J. *Chem. Soc., Faraday Trans.* **1996**, *92*, 4829.
- (15) Yim, W.-L.; Nowitzki, T.; Necke, M.; Schnars, H.; Nickut, P.; Biener, J.; Biener, M. M.; Zielasek, V.; Al-Shamery, K.; Klueener, T.; Baumer, M. J. *Phys. Chem. C* **2007**, *111*, 445.
- (16) Janssens, T. V. W.; Clausen, B. S.; Hvolvauk, B.; Falsig, H.; Christensen, C. H.; T.; Bligaard, T.; Norskov, J. K. *Top. Catal.* **2007**, *44*, 15.
- (17) Peters, K. F.; Steadman, P.; Isern, H.; Alvarez, J.; Ferrer, S. *Surf. Sci.* **2000**, *467*, 10.
- (18) Picollo, L.; Loffreda, D.; Cadet Santos Aires, F. J.; Deranlot, C.; Jugnet, Y.; Sautet, P.; Bertolini, J. C. *Surf. Sci.* **2004**, *566–568*, 995.
- (19) Pierce, M. S.; Chang, K.-C.; Hennessy, D. C.; Komanicky, V.; Menzel, A.; You, H. *J. Phys. Chem. C* **2008**, *112*, 2231.
- (20) The clean well-ordered Au(111) surfaces with typical herringbone reconstruction pattern were prepared by extensive Ne⁺ sputtering and high (~700 K) temperature annealing. The Au(111) surfaces with an extended step length were prepared by short (several minutes) 1 keV Ne⁺ sputtering at 400 K.
- (21) Hoffmann, F. M. *Surf. Sci. Reports* **1983**, *3*, 107.
- (22) Sanchez, A.; Abbet, S.; Heiz, U.; Schneider, W.-D.; Hakkinen, H.; Barnett, R. N.; Landman, U. *J. Phys. Chem. A* **1999**, *103*, 9573.
- (23) Winkler, C.; Carew, A. J.; Haq, S.; Raval, R. *Langmuir* **2003**, *19*, 717.
- (24) The DFT calculations were performed with the DMol3 codes, as detailed in ref 25. The DMol3 calculations used numerical basis sets and the PW91 descriptions of the exchange and correlation functionals. Slabs of four and nine atomic layers were utilized to model the Au(111) terrace, steps and kinks, respectively. Transition states here were identified using the combination of synchronous transit methods and eigenvector following and verified by the presence of a single imaginary frequency from a sequential vibrational frequency analysis.
- (25) Liu, P.; Rodriguez, J. A. *J. Chem. Phys.* **2007**, *126*, 164705.

JA8081268